Grirrane, A.; Alvarez-González, E.; García Gómez, H.; Corma Canós, A. (2017). Preparation of Tremorine and Gemini Surfactant Precursors with Cationic Ethynyl-Bridged Digold Catalysts. Chemistry - A European Journal. 23(12):2792-2801. doi:10.1002/chem.201605269

Catalytic Preparation of Tremorine and Gemini Surfactant Precursors via Cationic Ethynyl-Bridged Digold Intermediates

Abdessamad Grirrane[1], Eleuterio Álvarez[2], Hermenegildo Garcia[1] and Avelino Corma[1]

[1]Instituto Universitario de Tecnología Química CSIC-UPV, Univ. Politécnica de Valencia, Av. De los Naranjos s/n, 46022 Valencia (Spain) and [2]Instituto de Investigaciones Químicas CSIC-US, Departamento de Química Inorgánica, Av. Américo Vespucio 49, 41092 Sevilla (Spain).

Abstract: Tremorine and precursors of Gemini surfactants have been synthesized in one pot, three-steps, double catalytic A^3- coupling reaction and characterized by structural and spectroscopic properties. Cationic [Au(I)-L1][SbF_6] complex is more and extremely active catalyst compared to neutral L2 and L3- Au(I)-[bis(trifluoromethanesulfonyl)imidate] complexes (L1, L2 = Buchwald-type biaryl phosphane and L3 = triphenylphosphine) to promote the double A^3- coupling of ethyne, secondary amine (cyclic, aliphatic or aromatic) and formaldehyde. The solvent influences the catalytic performance by desilylation of silyl acetylene or deactivation of catalyst by halogen atom. Acetylide bridged cationic digold(I)-L1 and -L2 complexes have been isolated and characterized by single crystal XRD and spectroscopic properties. Iodine in the acetylene reagent deactivates the Au(I) catalyst by formation the less active iodide-bridged cationic digold(I)-L1 complex that was fully characterized by single crystal XRD and spectroscopic properties. Also it was observed that the nature of the phosphine ligand of the gold complexes used as catalyst affects the stability and activity of the formed cationic ethynyl-bridged di-Au(I)-L intermediates whose isolation lends support to the proposed double A^3-coupling mechanism.

Tremorine,[1] a symmetric pyrrolidinyl methyl acetylene [see structure in Table 1, Scheme (top)] is used to induce tremor in animals, allowing evaluation of the therapeutical activity of drugs for the treatment of Parkinson's disease. Gemini surfactants are structurally diverse type of symmetric amphiphilic compounds with two quaternary ammonium head groups connected through spacer [see structure in Table 2, Scheme (top)].[2] These compounds can be prepared from acetylene. However, the use of acetylene[3] in the laboratory is extremely hazardous due to its highly flammability and its intrinsic

instability, resulting in spontaneous explosion, especially when it is pressurized.[4] For this reason, it would be highly desirable to develop alternative synthetic procedures for tremorine and geminis surfactant precursors that not require acetylene manipulation. Surprisingly, however, there are no reports on catalytic processes for the synthesis these high-value compounds in one-pot multistep reaction involving a double A^3 coupling[5] in the two carbons of an ethynyl fragment. The known activity of homogeneous gold catalysts with [Au(I)-L][A] (L = phosphine and A = counterion) complexes[6] for the activation of numerous alkynes[5h, 5i, 7] has led us to anticipate that such complexes can also be efficient catalysts for the double A^3 coupling to synthesize tremorine and gemini surfactant precursors. In this regard, herein, we describe an efficient homogeneous gold (I) catalyst for the double A^3- coupling as new one-pot procedure for preparation tremorine and gemini surfactant precursors using ethynyltrimethylsilane (TMS-acetylene) as a safe ethynyl fragment, secondary amines (cyclic, aliphatic or aromatic) and formaldehyde. Other acetylene precursor, namely 1-iodo-2-(trimethylsilyl)acetylene, was also used in this study to shed light on the mechanism reaction.

In this work, two Au(I) complexes with Buchwald phosphanes, one cationic 2-di-tert-butylphosphanylbiphenyl (L1) and the other neutral 2-di-cyclohexyl phosphanyl -2',4',6'-triisopropylbiphenyl (L2) complexes (**1**) and (**2**) [Table 1, Scheme (Bottom)] have been tested as catalysts to promote the double A^3-coupling of ethynyltrimethylsilane (**4**), pyrrolidine (**5**) and formaldehyde (**6**). Their catalytic activity has been compared with that of the neutral triphenylphosphine (L3) Au^I complex (**3**)[8] [Table 1, Scheme (Bottom)]. Formation of 1-(3-(trimethylsilyl)prop-2-yn-1-yl)pyrrolidine (**7**) and 1-(prop-2-yn-1-yl)pyrrolidine (**8**) [Table 1, Scheme (Top)] as first and second product intermediates, respectively, and finally tremorine (**9**) was observed in high yield and selectivity, at low temperature [Table 1, Scheme (Top)]. One important conclusion from Table 1 (entries 1-3) is that the cationic Au^I complex (**1**) is more active in the presence of ethanol as solvent compared to toluene or CH_2Cl_2. This higher activity in ethanol can be explained by the faster desilylation[9] of TMS-protected alkyne (**7**) formed at the beginning as the first reaction intermediate by the OH-groups to form the terminal alkyne **8** as second reaction intermediate. Compound **8** finally reacts to give the targeted tremorine (**9**) [Table 1, Scheme (Top)]. Controls in the absence of any catalyst do not allow the detection of any product [Table 1 (entry 4)]. Tremorine (**9**) was characterized by NMR spectroscopy and GC-MS (see the experimental section and Figs. S1-S4 in

Supporting Information). ^{1}H, ^{13}C and Dept NMR spectra in CD_2Cl_2 provided evidence that the starting TMS-acetylene (**4**) and the intermediate compounds **7** and **8** are completely converted into tremorine (**9**). GC-MS data of **9** ($C_{12}H_{20}N_2$) shows a peak at 192.16 Da in agreement with the expected molecular formula (see Fig. S4 in the SI). The intermediate compounds **7** ($C_{10}H_{19}NSi$) and **8** ($C_7H_{11}N$) were also characterized during the kinetic study of this reaction by GC-MS showing peaks at 181.13 and 109.09 Da, respectively, in agreement with their expected molecular formulas (see Fig. S5 for **7** and Fig. S6 for **8** in the SI). The solid catalyst **1** can be recovered from the reaction mixture when ethanol is used as solvent and reused several times without losing activity and selectivity [Table 1 (entries 5-6)].

Table 1. One pot, double A^3- coupling reaction of TMS-acetylene (**4**), pyrrolidine (**5**), and formaldehyde (**6**) with complexes of Au(I) **1**, **2**, **3, 26,** (**26** + 1eq. of **$HSbF_6$**)**, 27,** (**27** + 1eq. of **$HNTf_2$**) or **31** as catalysts (6 mol %).[a]

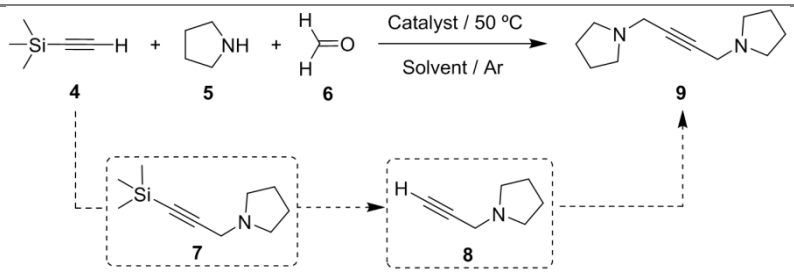

entry	Catalyst	Solvent	Time (h)	Conv. (%)[b]	Yield (%)[b] (**7** / **9**)
1	**1**	CH_2Cl_2	5	100	99 / 0
2	**1**	Toluene	5	100	99 / 0
3	**1**	Ethanol	2	100	0 / 99
4	**none**	Ethanol	5	0	0 / 0
5	**First reuse of 1**	Ethanol	2	100	0 / 99
6	**Second reuse of 1**	Ethanol	2	100	0 / 99
7	**2**	Ethanol	3	100	0 / 97
8	**3**	Ethanol	4	100	0 / 91
9	**26**[c]	Ethanol	4	100	0 / 96
10	**26**[c] **+ 1eq. of $HSbF_6$**[d]	Ethanol	2	100	0 / 99
11	**27**[c]	Ethanol	6	100	0 / 95
12	**27**[c] **+ 1eq. of $HNTf_6$**[e]	Ethanol	3	100	0 / 96
13	**31**	Ethanol	6	81	0 / 60[f]
14	**1**[g]	Ethanol	6	89	0 / 68[f]

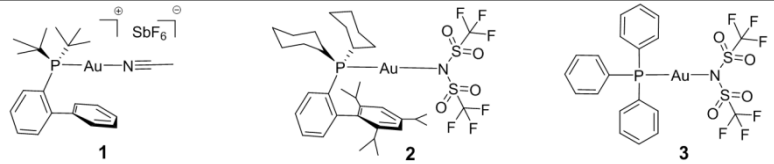

[a] Reactions were carried out using 0.25 mmol of TMS-acetylene, 0.7 of pyrrolidine and 1.4 mmol of aqueous formaldehyde and 1.5 ml of solvent. [b] conv. of **4** and yields (%) were determined by ^{1}H NMR spectroscopy and GC of the crude reaction mixture. [c] 3 mol % of di-Au(I) complex was used as catalyst. [d] 3 mol % of $HSbF_6$ acid was added. [e] 3 mol % of $HNTf_2$ acid was added. [f] 16 % of compound **8** are detected. [g] 0.25 mmol of 1-iodo-2-(trimethylsilyl)acetylene was used in the reaction instead of TMS-acetylene.

Under the optimal conditions, catalyst evaluation was extended to neutral complexes Au(I)-L2 (**2**) and Au(I)-L3 (**3**) [Table 1, Scheme (Bottom)]. Also in these cases tremorine (**9**) was obtained in good yield, but longer reaction times were required [Table 1 (entries 7-8)]. It was observed that the activity of the catalysts decreased in the order **1**, **2** to **3**. This catalytic activity order can be explained by the higher electrophilicity of Au(I) atom in cationic complex **1** respect to the neutral complexes **2** and **3**, and the higher structural stability of complex **2** compared with labile complex **3**. In the case of Au(I)-L3 (**3**) complex, it was observed that PPh_3 ligand is not able to stabilize the di-gold species formed during the catalytic reaction and decomposition[7b] takes place (see below).

To expand the scope of this catalytic process, ethynyltrimethylsilane (**4**) and aqueous formaldehyde (**6**) were reacted under optimal conditions, respectively, with 4-methylpiperidine (**10**), diisopropylamine (**14**), dibutylamine (**18**) and dibenzylamine (**22**) using the most active and stable cationic Au(I) complex **1** as catalyst (see Table 2). The expected reaction intermediates TMS-protected alkynes (**11**, **15**, **19** and **23**) and 1-(prop-2-yn-1-yl)amines (**12**, **16**, **20** and **24**) (see Table 2), were characterized during the kinetic studies of these reactions by GC-MS (see the experimental section and the Figs. S7-S14 in SI).

Table 2. One pot, double A^3- coupling reaction of TMS-acetylene, amines, and aqueous formaldehyde with complex of Au(I) **1** as catalysts (6 mol %).[a]

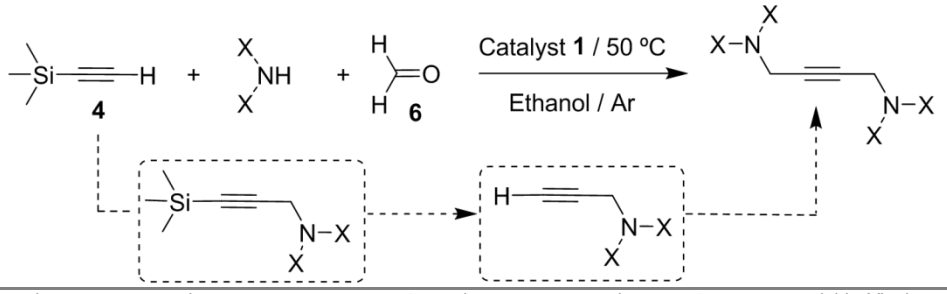

entry	Amine	First intermediate	Second intermediate	Time (h)	Conv. (%)[b]	Yield of final product (%)[b]
1	**10**	**11**	**12**	6	100	**13** (99)

2	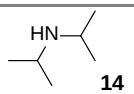 **14**	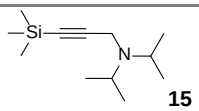 **15**	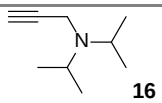 **16**	10	100	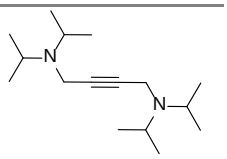 **17** (99)
3	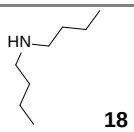 **18**	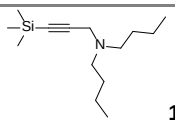 **19**	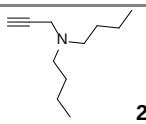 **20**	13	100	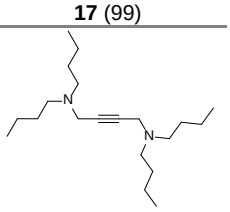 **21** (98)
4	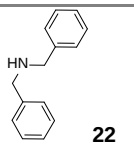 **22**	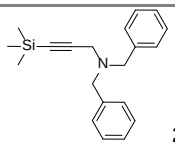 **23**	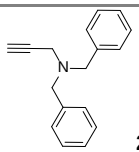 **24**	28	100	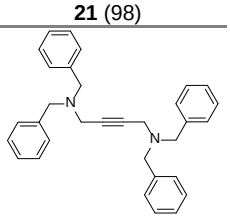 **25** (92)

[a] Reactions were carried out using 0.25 mmol of TMS-acetylene, 0.7 of amine and 1.4 mmol of aqueous formaldehyde and 1.5 ml of Ethanol. [b] conv. of **4** and yield of final products (%) were determined by ^{1}H NMR spectroscopy and GC of the crude reaction mixture.

The final wanted gemini surfactant precursors 1,4-bis(4-methylpiperidin-1-yl)but-2-yne (**13**), N,N,N´,N´-tetraisopropylbut-2-yne-1,4-diamine (**17**), N,N,N´,N´-tetrabutylbut-2-yne-1,4-diamine (**21**) and N,N,N´,N´-tetrabenzylbut-2-yne-1,4-diamine (**25**) (see Table 2) were isolated and characterized by ^{1}H, ^{13}C and Dept NMR spectroscopy (see Figs. S15-S17 for **13**, S19-S21 for **17**, S23-S25 for **21** and S27-S29 for **25** in the SI). GC-MS data obtained dissolving **13** ($C_{16}H_{28}N_2$), **17** ($C_{16}H_{32}N_2$), **21** ($C_{20}H_{40}N_2$) and **25** ($C_{32}H_{32}N_2$) in CH_2Cl_2 show peaks at 248.3, 252.3, 308.2 and 444.2 Da, respectively, in agreement with the expected molecular formulae (see Figs. S18, S22, S26 and S30, respectively, in the SI).

The solid state structure of **25** was confirmed by single-crystal X-ray diffraction (For X-ray data, ortep view and crystal packing details see, Table S1 and Fig. S31 in the SI). Also high quality crystals of protonated salt **13a** suitable for single crystal X-ray diffraction were obtained by adding 2 eq. of aqueous HCl (37 %) over the solution of compound **13** in CH_2Cl_2 at RT allowing the biphasic mixture to equilibrate. The solid state structure confirms the double protonation of compound **13** with the presence of two chlorine atoms as counterion, leading to the dipositive salt **13a** (For X-ray data, ortep view and crystal packing details see Table S2 and Fig. S32 in the SI). Following the same procedure dipositive salt **17a** was obtained and confirmed by elemental analysis and ^{1}H, ^{13}C and

Dept NMR spectroscopy in deuterated DMSO (see Figs. S33-S35 in the SI) providing evidence that compound **17** is completely converted into double protonated salt **17a**.

Besides Gemini surfactant precursors **13**, **17**, **21** and **25**, formation of TMS-protected-alkynes **11** ($C_{12}H_{23}NSi$), **15** ($C_{12}H_{25}NSi$), **19** ($C_{14}H_{29}NSi$) and **23** ($C_{20}H_{25}NSi$) was observed as primary products at the initial stages of the reactions (see Table 2). These reaction intermediates were characterized by GC-MS data showing a peak at 209.2, 211.2, 239.2 and 307.3 Da, respectively, in agreement with their expected molecular formulae (see Figs. S7, S9, S11 and S13 in the SI). Subsequent desilylation of compounds **11**, **15**, **19** and **23** leads to the corresponding terminal alkynes, i.e., 4-methyl-1-(prop-2-yn-1-yl)piperidine (**12**), N,N-diisopropylprop-2-yn-1-amine (**16**), N-butyl-N-(prop-2-yn-1-yl)butan-1-amine (**20**) and N,N-dibenzylprop-2-yn-1-amine (**24**) as second reaction intermediates in the formation of Gemini surfactant precursors (see Table 2). These terminal alkynamines were also characterized by GC-MS data showing peaks at 137.2, 139.3 , 167.3 and 235.3 Da in agreement with the expected molecular formulae **12** ($C_9H_{15}N$), **16** ($C_9H_{17}N$), **20** ($C_{11}H_{21}N$) and **24** ($C_{17}H_{17}N$) (see Figs. S8, S10, S12 and S14 in the SI).

In an attempt to isolate some Au^I complexes that could shed light on the reaction mechanism for the formation of these Gemini surfactant precursors obtained in one pot, double A^3-coupling using gold (I) complexes as catalysts, several experiments were done. In one of them, we proceeded to react a stoichiometric (3:1) mixture of ethynyltrimethylsilane (**4**) with gold (I) complexes **1** and **2** in dry CH_2Cl_2 at RT for 24 h and 60 ºC for 72 h, respectively (Scheme 1). Filtration of the resulting dark solutions followed by addition of n-hexane at -30 ºC or RT lead to the formation of colourless needles crystals of the air stable cationic di-gold (I) acetylide complexes[7a, 7b, 10] of **26** and **27**, respectively, in good isolated yields respect to the initial complexes **2** and **3** (86 and 71 %). Complexes **26** and **27** were fully characterized by analytical and spectroscopic data (see the Experimental Section, Table S3-S4 and Figs. S36-S48 in the SI).

^1H, ^{13}C, and ^{31}P NMR spectroscopy of CD_2Cl_2 solutions provides evidence showing that under the reaction condition the starting complexes **1** and **2** are completely converted into the corresponding cationic di-gold (I) acetylide complexes of **26** and **27**, releasing $Me_3Si\text{-}SbF_6$[11] and $Me_3Si\text{-}NTf_2$ adducts, respectively (see Figs. S36-S39 for **26** and S41-S42 for **27** in the SI). Thus, ^{31}P NMR spectroscopy shows the appearance of

new peaks at δ = 62.46 and 38.74 ppm corresponding to **26** and **27**, respectively (see Figs. S39 and S45 in the SI). These peaks are different from those recorded in ^{31}P NMR spectroscopy for the original Au(I) complexes **1** (57.49 ppm) and **2** (33.29 ppm). Cationic bridged-acetylide di-gold (I) complexes **26** and **27** (Scheme 1) are fluxional in solution and exhibit at room temperature a single $^{31}P\{^{1}H\}$ resonance. Similarly to ^{31}P NMR, ^{1}H NMR spectroscopy also shows new signals of methyl groups for complex **26** at 1.37/1.32 instead of 1.38/1.33 ppm corresponding to the initial complex **1** and for complex **27** at 1.32/1.22/0.93 instead of 1.38/1.21/0.90 ppm corresponding to the initial complex **2** (See Fig.S36 for **26** and Fig.S44 for **27** in the SI). The ethynyl bridge in the σ,π-acetylide complex **26** exhibits $^{13}C\{^{1}H\}$ resonances at 138.52 (t, $^{2}J_{CP}$ = 64.34 Hz) and 96.37 ppm (t, $^{3}J_{CP}$ = 15.17 Hz) (See Fig. S37 in the SI), which are due to the C and CH moieties of bridging ethynyl ligand (C≡CH) as confirmed by Dept.135, HMQC and COSY -NMR experiments (see Figs. S38, S40 and S41, respectively, in the SI). Recently, it was published the first cationic ethynyl-bridge di-gold(I) complex stabilized by bulky terphenyl phosphine ligand using hydrocarbonyl transfer reagent [Mg(C≡CH)X; X = Cl, Br] as precursor of ethynyl fragment.[12]

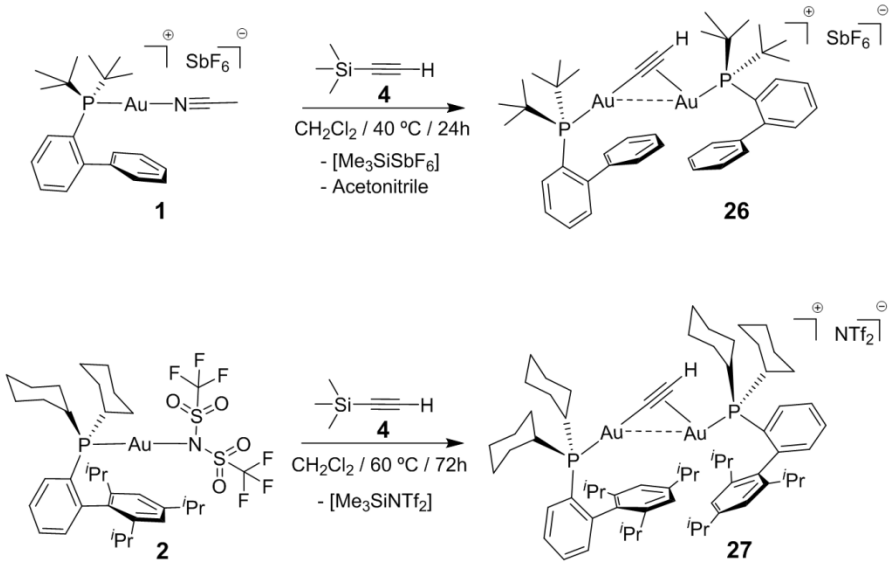

Scheme 1. Synthesis of the cationic bridged-acetylide di-gold (I) complexes **26** and **27**.

ESI-MS of solutions obtained after dissolving fluxional cationic [(σ,π)](L1-Au)$_2$(μ-acetylene)[SbF_6] (**26**) and [(σ,π)](L2-Au)$_2$(μ-acetylene)[NTf_2] (**27**) complexes,

respectively, in CH_2Cl_2 showed intense positive MS peaks at 1015.3 and 1371.9 Da (see Fig. S42 for **26** and Fig. S47 for **27** in the SI) that are attributable, respectively, to the cationic $[C_{42}H_{55}Au_2F_6P_2Sb$ (**26**) - $SbF_6^-]^+$ and $[C_{70}H_{99}Au_2F_6NO_4P_2S_2$ (**27**) - $N(SO_2CF_3)_2^-]^+$ species, that are also in good agreement with the simulated isotopic distributions for the molecular formula $[C_{42}H_{55}Au_2P_2]$ and $[C_{68}H_{99}Au_2P_2]$, respectively (See Fig. S42 for **26** and Fig. S47 for **27** in the SI). Two negative MS peaks were found in the case of complex **26** at 234.6 and 236.6 Da corresponding to the two isotopes ^{121}Sb and ^{123}Sb of $[SbF_6]^-$ counter anion (See Fig. S42 in the SI), versus single negative MS peak at 279.7 Da corresponding to $[N(SO_2CF_3)_2]^-$ counter anion of complex **27** (See Fig. S47 in the SI).

The molecular structure of complexes **26** and **27** (Scheme 1) was confirmed by single-crystal X-ray diffraction. ORTEP structures of complexes **26** and **27** are shown in Figure 1 (For X-ray data, ortep view and crystal packing details see in the SI: Table S3 and Fig.S43 for **26** and Table S4 and Fig.S48 for **27**). In both complexes, carbon atom C1 of bridged-acetylene is bonded to the two gold atoms in a non-symmetric and symmetric fashion, respectively, with the Au1-C1 and Au1A-C1 distance of 2.006(4) and 2.138(6) Å, respectively, for **26** and **27**, bonds being shorter and equal than Au2-C1 and Au1-C1 with distances about 2.309(4) and 2.138(6) Å, respectively, for **26** and **27**. In both complexes, Au2 and Au1 atoms are also bonded to the terminal ethynyl carbon atom C2 with the Au2-C2 and Au1-C2 distance of 2.194(5) and 2.418(6) Å, respectively, for **26** and **27**. The aurophilic bonding Au1-Au2 and Au1-Au1A in **26** and **27** is about 3.679 and 3.638 Å, respectively.

The catalytic activity of cationic di-gold $[(\sigma,\pi)](L1\text{-}Au)_2(\mu\text{-acetylene})[SbF_6]$ (**26**) complex was also tested for the double A^3 coupling of ethynyltrimethylsilane (**4**), pyrrolidine (**5**) and formaldehyde (**6**), whereby tremorine (**9**) was obtained in good yield, but needing longer reaction time (Table 1, entry 9) compared to the cationic complex **1** (Table 1, entry 3). We found that when 1 eq. of $HSbF_6$ is added to the di-gold complex **26** in the catalytic double A^3-coupling, a higher reaction rate for the formation of tremorine (**9**) is observed (Table 1, entry 10) and the result in this case is similar than when cationic complex **1** is used as pre-catalyst (Table 1, entry 3). The role of this equivalent of acid is justified in our mechanistic proposal (Scheme 3) in the absence of CH_2Cl_2.[5i] Also the catalytic activity of cationic di-gold $[(\sigma,\pi)](L2\text{-}Au)_2(\mu\text{-acetylene})[NTf_2]$ (**27**) and its mixture with 1 eq. of $HNTf_6$ acid were measured (Table 1,

entries 11 and 12, respectively), the results following the same trend as the previously commented experiments of complex **26**.

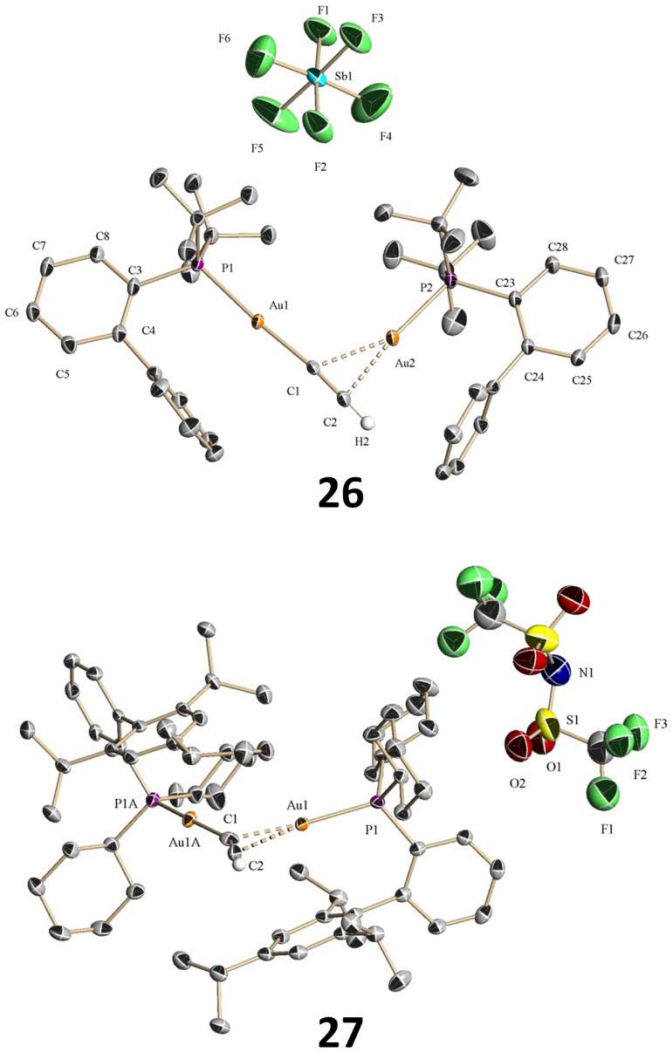

Figure 1. ORTEP views of cationic bridged-acetylide di-gold (I) complexes **26** and **27**; hydrogen are omitted for clarity, and thermal ellipsoids are set at 30 % probability level (single-crystal X-ray data and crystal packing details are given in Table S3 and Fig.S43 for **26** and Table S4 and Fig.S48 for **27** in the SI).

Another additional unsuccessful experiment aimed to isolate the di-gold (I) acetylide complex (**28**) (Scheme 2, top) was performed by using the same conditions as those used in the formation of complexes **26** and **27** (Scheme 1), but using in this case a stoichiometric (1:3) mixture of gold (I) complex **3** with ethynyltrimethylsilane (**4**), in dry CH_2Cl_2 at RT for 24 h (Scheme 2). A black precipitate was formed. This precipitate could

be collected by filtration to be analysed by HR-TEM, DF-STEM and EDX-analysis after sonication in DCE (see below), addition of toluene to the collected transparent supernatant solution and slow crystallization at RT, leading to the formation of pure cationic complex [Au(I)-(PPh_3)$_2$][$N(SO_2CF_3)_2$] (**30**) (Scheme 2, top) in 46 % yield. Complex **30** has been previously reported by us[7b] as being formed in a different reaction (see the experimental section in the SI). Complex **30** was fully characterized by ^{1}H, ^{13}C, dept.135, ^{31}P and ^{19}F NMR spectroscopy (see, Figs. S49-S53 in the SI), ESI-MS (see, Fig. S54 in the SI), combustion analysis and by single-crystal X-ray crystallography (see, Figs. S55 in the SI). The structure obtained here resulting identical to the one previously published for **30**.[7b]

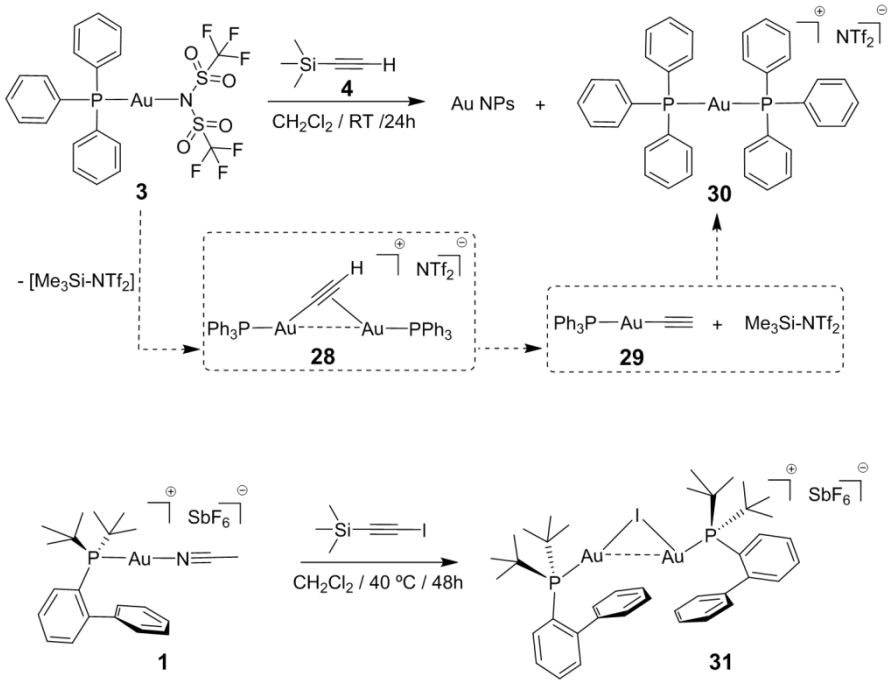

Scheme 2. Top: Failure to isolate any Au(I) acetylide complex and formation of Au NPs and cationic Au(I) complex **30**. Bottom: deactivation of cationic Au(I) complex **1** by formation of a less active, cationic bridged iodide digold(I) [(L1Au)$_2$(μ-I)][SbF_6] (**31**) complex when 1-iodo-2-(trimethylsilyl)acetylene is used as reagent instead of ethynyltrimethylsilane (**4**).

The HR-TEM and DF-STEM images together with the EDX-analysis of this black solid reveal the formation of well dispersed homogeneous Au NPs with diameter between 1 and 3 nm [See Figure 2 (Top) and Figs. S56-S57 in the SI for more details]. Note that this experiment is similar to the previously published one[7b] in which phenylacetylene was

used as reagent instead of ethynyltrimethylsilane (**4**), but in the present case no alkyne gold (I) complexes such as **28** and **29** (Scheme 2, top) were detected probably due the quick decomposition of the presumed cationic [(σ,π)(PPh_3-Au)$_2$(μ-acetylene)][NTf_2] (**28**) and neutral [(σ)(PPh_3-Au)(acetylene)] (**29**) (Scheme 2, top). The easy decomposition of presumed complexes **28** and **29** can be explained considering that it is known[7a, 7b] that the less bulky PPh_3 ligand has low ability to stabilize such (μ-acetylene)[(σ,π)]digold-system compared with the sterically encumbered phosphine ligands L1 and L2 present, respectively, in **26** and **27** (Scheme 1). Thus, the mixture of gold (I) complex **3** with ethynyltrimethylsilane (**4**) in CD_2Cl_2 at RT was followed by ^{31}P NMR spectroscopy providing evidence that the starting gold (I) complex **3** (30.48 ppm) was completely converted into complex **30** (45.09 ppm) over the time (see Figs. S58-S60 in the SI). ^{31}P NMR spectroscopy shows the appearance at 5 min reaction time of a minor (1 %) new peak at (45.09 ppm) corresponding to complex **30** versus a major (99 %) peak of starting complex **3** (see Fig. S58 in the SI). Over the time (30 min) complex **3** disappeared completely, accompanied by the appearance of a new peak at 36.50 ppm (92 %) attributable to a presumed σ-acetylide gold(I) complex **29**, similarly to the previously isolated σ-phenylacetylide gold(I) complex,[7b] together with 8 % of complex **30** (45.09 ppm) (see Fig. S59 in the SI). At 2 h reaction time, complex **30** was almost (99 %) the only product detectable, with a remaining trace (less than 1%) amount of acetylide gold(I) complexes mono-gold **28** (32.80 ppm) and di-gold **29** (36.60 ppm) (see Fig. S60 in the SI).

In another experiment, 1-iodo-2-(trimethylsilyl)acetylene was used as reagent instead of ethynyltrimethylsilane (**4**) to react with gold (I) complex **1**, in a (3:1) stoichiometric mixture, in dry CH_2Cl_2 at RT and 40 ºC for 48 h (Scheme 2, bottom). Filtration of the resulting dark solution followed by addition of n-hexane at -30 ºC lead to the formation of colourless crystals of the air stable cationic bridged iodide di-gold (I) [(L1-Au)$_2$(μ-I)[SbF_6] (**31**) complex in good isolated yield respect to the initial complex **1** (92 %). The di-gold(I) complex **31** was characterized by NMR spectroscopy and ESI-MS (see the experimental section and Figs. S61-S65 in the SI). ^{1}H, ^{13}C, Dept.135 and ^{31}P NMR spectra in CD_2Cl_2 provided evidence that the starting gold (I) complex **1** was completely converted into complex **31** (see Figs. S61-S64 in the SI). Thus, ^{31}P NMR spectroscopy shows the appearance of a new peak at δ = 66.58 ppm, attributable to **31** (see Fig. S64 in

the SI). This peak is different from the one recorded in ^{31}P NMR spectroscopy for the original complex **1** (57.49 ppm).

ESI-MS of the solution obtained after dissolving, cationic $[(L1\text{-}Au)_2(\mu\text{-}I)][SbF_6]$ (**31**) complex in CH_2Cl_2 showed an intense positive MS peak at 1117.3 Da (see Fig. S65 in the SI) that is attributable to the cationic $[C_{40}H_{54}Au_2F_6IP_2Sb$ (**31**) - $SbF_6^-]^+$ species whose isotopic distribution is in good agreement with the simulated isotopic distribution for the molecular formula $[C_{40}H_{54}Au_2IP_2]$ (see details in Fig. S65 in the SI). Negative MS exhibits mainly single cluster at 234.6 and 236.6 Da attributable to counter-anion SbF_6^- of complex **31** with the ^{121}Sb and ^{123}Sb isomers (see Fig. S65 in the SI). Combustion elemental analysis of complex **31** was also in accordance with the percentages expected for its molecular formula (see experimental section in the SI).

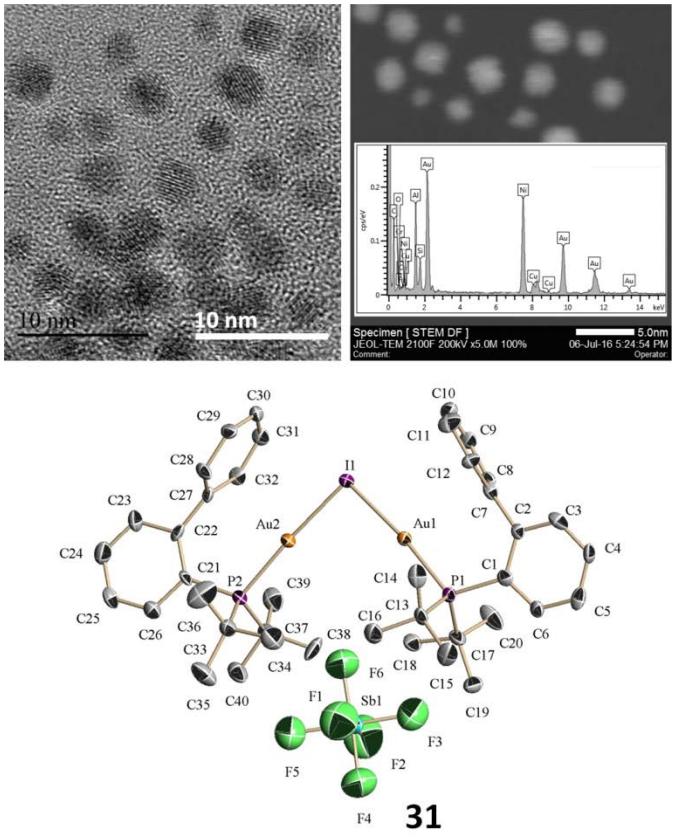

Figure 2. Top: HR-TEM and DF-STEM images as well as EDX analysis of well dispersed homogeneous Au NPs with diameter between 1-3 nm obtained in the reaction of complex **3** and acetylene **4**. Bottom: ORTEP view of complex **31**; ellipsoids are given at the 30 % probability level (single-crystal X-ray data and crystal packing details are given in Table S5 and Fig. S66 in the SI).

The molecular structure of complex **31** [Scheme 2 (Bottom)] was confirmed by single-crystal XRD, the ORTEP structure of **31** complex is shown in Figure 2 (Bottom) (See, Table S5 and Figs. S66 for details in the SI). In this complex, iodide atom is bonded to the two gold atoms in a symmetric fashion, with the Au1-I1 and Au2-I1 distance of 2.5895(8) and 2.5888(8) Å. The aurophilic Au1-Au2 bonding for **31** is about 3.837 Å, being this bond longer than the Au1-Au2 and Au1-Au1A bonds in complexes **26** and **27** that are 3.679 and 3.638 Å, respectively.

The catalytic activity of this cationic iodide bridged di-gold(I) $[(L1\text{-}Au)_2(\mu\text{-}I)][SbF_6]$ (**31**) complex was tested for the preparation of tremorine (**9**) (Table 1, entry 13), the result confirming its low activity. This low activity was also observed when gold (I) complex **1** is used as catalyst, but using 1-iodo-2-(trimethylsilyl)acetylene as reagent instead of ethynyltrimethylsilane (**4**). It is very likely that using iodo acetylene as reagent, deactivation of gold (I) complex **1** occurs due to reaction with iodide atoms released to the medium and leading to the formation of the less active cationic iodide bridged di-gold(I) **31** complex (Table 1, entry 14).

In order to shed light in to the reaction mechanism and also to gain understanding on the implication of acetylide di-gold (I) complexes **26** and **27** in catalysis, the reaction of ethynyltrimethylsilane (**4**), pyrrolidine (**5**) and formaldehyde (**6**) using bulky gold complex **2** as precatalyst was followed by ^{1}H, ^{31}P NMR and ESI-MS spectroscopy. In the first step, 15 mol % of gold complex **2** was added to ethynyltrimethylsilane (**4**), whereby ^{31}P NMR spectroscopy shows a new peak at 38.48 ppm matching with the chemical shit of cationic acetylide-bridged di-gold (I) complex **27**, together with the peak corresponding to original complex **2** (33.37 ppm) in CD_2Cl_2 (See Fig. S68 for details in the SI). Also ^{1}H NMR spectroscopy and ESI-MS confirm the coexistence of the two complexes **2** and **27** in the isolated solid catalyst during the first stage of reaction at 3 h reaction time (See Fig. S67 for ^{1}H-NMR and Fig. S69 for ESI-MS spectra in the SI). It should be commented that from this mixture of complexes, we have been able to isolate crystals of complex **2** with quality enough to be analysed by single crystal XRD, resulting in a new solid structure of this complex (ORTEP, crystal packing details and X-ray data are given in Table S6 and Fig. S70 in the SI). Over the time (12 h) complex **2** completely disappeared, remaining exclusively the di-gold (I) complex **27** and releasing one equivalent of $Me_3Si\text{-}NTf_2$ to the reaction medium (See Figs. S71-S73 for ^{1}H, ^{31}P and ^{19}F NMR spectra in the SI). In a second step of this catalytic process, pyrrolidine (**5**),

formaldehyde (**6**) and 0.5 ml of ethanol were added over the mixture and the changes were followed again by NMR spectroscopy. After 1 h, the mixture was analysed by ^{31}P NMR spectroscopy, showing the total disappearance of a peak at 38.48 ppm corresponding to cationic acetylide-bridged di-gold (I) intermediate **27** (See, Fig. S74 in the SI) and the formation of new peaks at 33.63, 33.68, 35.17 and 44.39 ppm attributable to proposed cationic nitrogenated gold(I) complexes **32**, **33**, **34** and **35** (Scheme 3). In addition, other two peaks at 35.73 and 43.81 ppm were also observed attributable, respectively, to a total (neutral chlorine gold(I) L2-Au-Cl) and partially (cationic chloride-bridged di-gold(I) $[(L2\text{-}Au)_2(\mu\text{-}Cl)][NTf_2]$)[13] deactivated forms of gold(I) complexes,[5i] originated by the use as solvent of CD_2Cl_2 in the presence of pyrrolidine (**5**). Over the time (5 h), the peaks corresponding to active catalytic intermediates (33.63, 33.68, 35.17 and 44.39 ppm) were gradually consumed (See, Fig. S75 in the SI) and after 12 h reaction time, the only observed species was the deactivated chlorine-Au(I) complexes with ^{31}P NMR spectroscopy peaks at 35.75 and 43.59 ppm (See, Fig. S76 in the SI).

Based on these spectroscopic observations, a plausible reaction mechanism[5g-i, 14] for the one pot, double A^3- coupling of ethynyl, pyrrolidine and formaldehyde using bulky L1- or L2- gold(I) complexes as precatalyst in the absence of CH_2Cl_2 can be proposed (Scheme 3). The main feature of this mechanism is the coordination of Au(I) precatalyst **1** or **2** with the ethynyl group leading to the isolated cationic acetylide-bridged di-gold (I) complexes $[(\sigma,\pi)](L1\text{-}Au)_2(\mu\text{-acetylene})[SbF_6]$ (**26**) or $[(\sigma,\pi)](L2\text{-}Au)_2(\mu\text{-acetylene})[NTf_2]$ (**27**) as catalytic intermediates, releasing to the medium $Me_3Si\text{-}SbF_6$ or $Me_3Si\text{-}NTf_2$ adducts that can be converted in the presence of ethanol as solvent to the corresponding acids $HSbF_6$ or HTf_2 and ethoxytrimethylsilane. The condensation reaction between formaldehyde and pyrrolidine would take place spontaneously or catalysed by acids. The presumed π-complexes intermediates **32** and **33** involved in the mechanism (see Scheme 3) formed between gold and ethynyltrimethylsilane (**4**) or ethynyl, will undergo N-ligand exchange to from the 1-(3-(trimethylsilyl)prop-2-yn-1-yl)pyrrolidine (**7**) and 1-(prop-2-yn-1-yl)pyrrolidine (**8**) as first and second reaction intermediates. This ligand exchange will give rise to the formation of $[Au(L1)(pyrrolidine)][SbF_6]$ (**34**)[5i] as catalytic complex intermediate. Subsequent reaction of gold(I) π-complex **33**, gold(I) complex **34** and formaldehyde (**6**) leads to the formation of a presumed di-cationic $[(L1\text{-}Au)_2(\mu\text{-tremorine})][(SbF_6)_2]$ (**35**) complex

closely related to our previous isolated di-copper(I) complex.[5h] In the last step, tremorine (**9**) as final product would be formed by exchange from the coordination sphere of the two atoms of Au(I) from di-gold(I) complex **35** by replacement with free pyrrolidine present in the reaction medium and regeneration [Au(L1)(pyrrolidine)][SbF_6] (**34**) complex that can start over other cycles of this catalytic reaction.

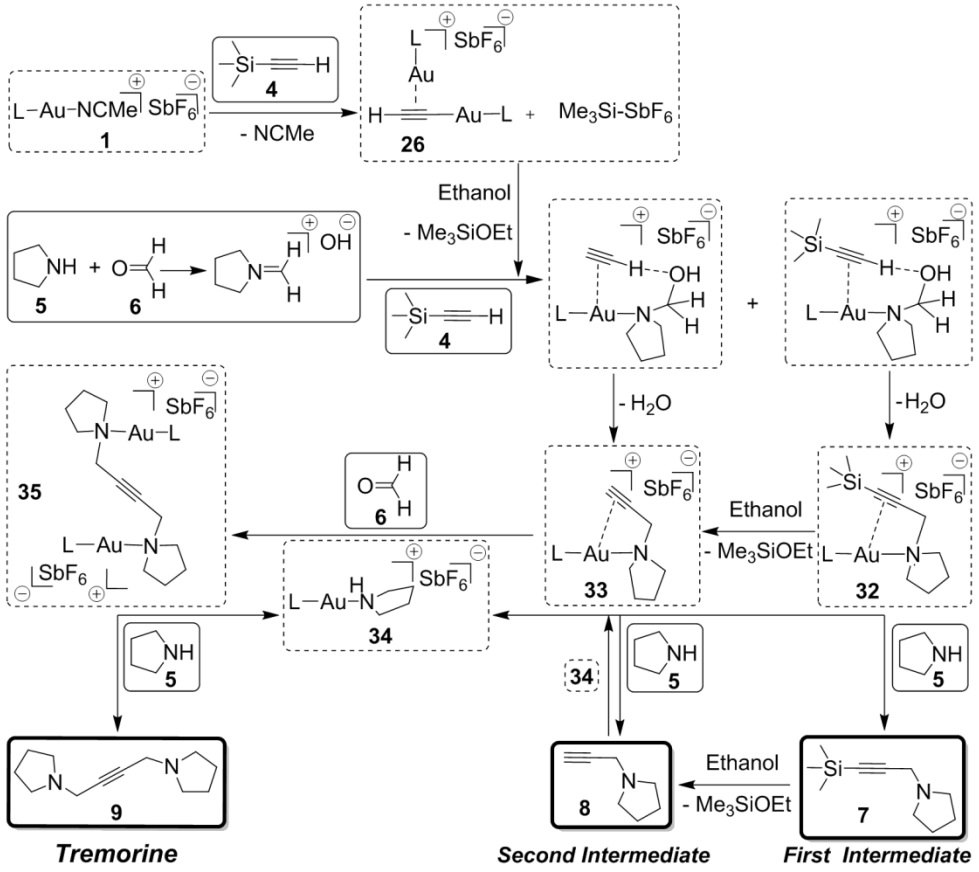

Scheme 3. Plausible mechanism for one pot, double A^3- coupling of ethynyl, secondary amine and formaldehyde using cationic gold(I) complex **1** as precatalyst in ethanol. Pyrrolidine (**5**) was choosen as model of secondary amine, resulting in the formation of tremorine (**9**).

This manuscript has shown the synthesis of tremorine and gemini surfactant precursors through a catalytic one pot, double A^3-coupling reaction. The reaction products have been fully characterized by their structural and spectroscopic properties. It was observed that the nature of the phosphine ligand (L1, L2 or L3) present in the gold complexes used as catalyst affects the stability and activity of the formed cationic ethynyl-bridged di-Au(I)-L complexes involved in the reaction mechanism intermediates. The activity data show

the possible ways in which the solvent can influence the catalyst performance by limiting the extent of desilylation of acetylene reagents. The presence of iodine in the acetylene reagent results on the partial deactivation of the Au(I) catalyst by formation the iodide-bridged cationic digold(I)-L1 complex that was fully characterized by structural and spectroscopic properties. Unsubstituted acetylide unit-bridged cationic digold(I)-L1 and -L2 complexes have been isolated, characterized by structural and spectroscopic properties and their role as intermediates in the reaction mechanism supported by control experiments.

Experimental

ESI contains experimental details describing the synthesis, isolation, analytical and spectroscopic data of tremorine and gemini surfactant precursors **9** and **13**, **13a**, **17**, **17a**, **21**, **25**, as well as new gold(I) complexes **26**, **27** and **31**, including NMR spectra, combustion analysis, GC-MS, ESI-MS, HR-TEM, STEM-DF, EDX-analysis and X-ray crystallography data. ESI also contains full crystallographic data of X-ray structures for: **2** (CCDC-XXXXXX), **13a** (CCDC-XXXXXX), **25** (XXXXXX), **26** (XXXXXX), **27** (XXXXXX) and **31** (XXXXXX). These data can also be obtained free of charge from The Cambridge Crystallographic Data centre via http//www.ccdc.cam.ac.uk/data_request/cif.

Acknowledgements

Financial support by the Spanish Ministry of Economy and Competitiveness (Severo Ochoa and CTQ2015-69153-CO_2-R1) and Generalidad Valenciana (Prometeo 2013-014) is gratefully acknowledged.

References

[1] aA. K. Cho, W. L. Haslett, D. J. Jenden, *Biochem. Biophys. Res. Commun.* **1961**, *5*, 276-279; bF. M. Menger, J. S. Keiper, V. Azov, *Langmuir* **2000**, *16*, 2062-2067; cG. M. Everett, L. E. Blockus, I. M. Shepperd, *Science (Washington, DC, U. S.)* **1956**, *124*, 79.

[2] aL. C. S. L. Morais, L. J. Quintans-Junior, C. I. F. Franco, J. R. G. S. Almeida, R. N. Almeida, *Pharmacol., Biochem. Behav.* **2004**, *79*, 745-749; bH. Szmigielska, A. Szmigielski, A. Szadowska, *Pol. J. Pharmacol.* **1993**, *45*, 291-298; cV. Dutt Sharma, M. A. Ilies, *Med. Res. Rev.* **2014**, *34*, 1-44.

[3] aJ. N. Wilson, S. M. Waybright, K. McAlpine, U. H. F. Bunz, *Macromolecules* **2002**, *35*, 3799-3800; bC.-J. Li, W. T. I. V. Slaven, C.-J. Li, Y.-P. Chen, V. T. John, S. H. Rachakonda, *Chem. Commun. (Cambridge)* **1998**, 1351-1352.

[4] aC. R. Gillett, O. S. Hellwig, *ACETYLENE-GAS GENERATOR* **1898**, *US603506A*, CAPLUS AN 1906:71268(Patent); bA. Rosenberg, *APPARATUS FOR THE GENERATION OF ACETYLENE GAS* **1906**, *US824509A*, CAPLUS AN 1906:52518(Patent).

[5] aC. Wei, C.-J. Li, *J. Am. Chem. Soc.* **2003**, *125*, 9584-9585; bC. Wei, Z. Li, C.-J. Li, *Synlett* **2004**, 1472-1483; cB. Yan, Y. Liu, *Org. Lett.* **2007**, *9*, 4323-4326; dJ. Li, L. Liu, D. Ding, J. Sun, Y. Ji, J. Dong, *Org. Lett.* **2013**, *15*, 2884-2887; eS. Shi, T. Wang, V. Weingand, M. Rudolph, A. S. K. Hashmi, *Angew. Chem., Int. Ed.* **2014**, *53*, 1148-1151; fJ. Li, M. Rudolph, F. Rominger, J. Xie, A. S. K. Hashmi, *Adv. Synth. Catal.* **2016**, *358*, 207-211; gA. Grirrane, E. Alvarez, H. Garcia, A. Corma, *Chem. - Eur. J.* **2016**, *22*, 340-354; hA. Grirrane, E. Alvarez, H. Garcia, A. Corma, *Chem. - Eur. J.* **2014**, *20*, 14317-14328; iA. Grirrane, E. Alvarez, H. Garcia, A. Corma, *Angew. Chem., Int. Ed.* **2014**, *53*, 7253-7258.

[6] aA. Stephen, K. Hashmi, G. J. Hutchings, *Angew. Chem., Int. Ed.* **2006**, *45*, 7896-7936; bA. Arcadi, *Chem. Rev. (Washington, DC, U. S.)* **2008**, *108*, 3266-3325; cS. Diez-Gonzalez, N. Marion, S. P. Nolan, *Chem. Rev. (Washington, DC, U. S.)* **2009**, *109*, 3612-3676; dD. J. Gorin, B. D. Sherry, F. D. Toste, *Chem. Rev. (Washington, DC, U. S.)* **2008**, *108*, 3351-3378; eA. Fuerstner, P. W. Davies, *Angew. Chem., Int. Ed.* **2007**, *46*, 3410-3449; fD. Pflaesterer, A. S. K. Hashmi, *Chem. Soc. Rev.* **2016**, *45*, 1331-1367.

[7] aA. Grirrane, H. Garcia, A. Corma, E. Alvarez, *ACS Catal.* **2011**, *1*, 1647-1653; bA. Grirrane, H. Garcia, A. Corma, E. Alvarez, *Chem. - Eur. J.* **2013**, *19*, 12239-12244; cR. E. M. Brooner, R. A. Widenhoefer, *Angew. Chem., Int. Ed.* **2013**, *52*, 11714-11724; dA. M. Asiri, A. S. K. Hashmi, *Chem. Soc. Rev.* **2016**, *45*, 4471-4503.

[8] N. Mezailles, L. Ricard, F. Gagosz, *Org. Lett.* **2005**, *7*, 4133-4136.

[9] aA. S. K. Hashmi, E. Kurpejovic, W. Frey, J. W. Bats, *Tetrahedron* **2007**, *63*, 5879-5885; bA. Zeiler, M. J. Ziegler, M. Rudolph, F. Rominger, A. S. K. Hashmi, *Adv. Synth. Catal.* **2015**, *357*, 1507-1514.

[10] aA. S. K. Hashmi, T. Lauterbach, P. Noesel, M. H. Vilhelmsen, M. Rudolph, F. Rominger, *Chem. - Eur. J.* **2013**, *19*, 1058-1065; bA. S. K. Hashmi, I. Braun, P. Noesel, J. Schaedlich, M. Wieteck, M. Rudolph, F. Rominger, *Angew. Chem., Int. Ed.* **2012**, *51*, 4456-4460, S4456/4451-S4456/4430; cI. Braun, A. M. Asiri, A. S. K. Hashmi, *ACS Catal.* **2013**, *3*, 1902-1907.

[11] G. A. Olah, L. Heiliger, X. Y. Li, G. K. S. Prakash, *J. Am. Chem. Soc.* **1990**, *112*, 5991-5995.

[12] M. F. Espada, J. Campos, J. Lopez-Serrano, M. L. Poveda, E. Carmona, *Angew. Chem., Int. Ed.* **2015**, *54*, 15379-15384.

[13] A. Zhdanko, M. Stroebele, M. E. Maier, *Chem. - Eur. J.* **2012**, *18*, 14732-14744, S14732/14731-S14732/14102.

[14] A. S. K. Hashmi, *Angew. Chem., Int. Ed.* **2010**, *49*, 5232-5241.